Original scientific paper

DESIGNING AN EFFICIENT OBSERVER FOR THE NON-LINEAR LIPSCHITZ SYSTEM TO TROUBLESHOOT AND DETECT SECONDARY FAULTS CONSIDERING LINEARIZING THE DYNAMIC ERROR

Hamed Mobki[1], Morteza Homayoun Sadeghi[2], Aydin Azizi[3], Mir Mohammad Eskandari[4]

[1]Center of Condition Monitoring at Urmia Combined Cycle Power Plant, West Azerbaijan Power Generation Management Company, Iran
[2]Department of Mechanical Engineering, University of Tabriz, Iran
[3]School of Engineering, Computing and Mathematics, Oxford Brookes University, United Kingdom
[4]Department of Mechanical Engineering, University of Tehran, Iran

Abstract. *The presence of faults in a system leads to a lower value for efficiency, accuracy and speed, and, in some cases, even a complete breakdown. Thus, early fault detection is a major factor in efficiency and productivity of the procedure. In recent decades, many research studies have been conducted on troubleshooting and secondary fault detection. The current work presents an efficient and novel observer design capable of stabilizing the residue and dynamic error for the nonlinear Lipschitz systems with faults as well as a troubleshooting analysis and determining the formation of secondary faults in defective systems. The observer is designed based on linearizing dynamic error considering uncertainty, disturbance, and defects by employing non-linear gain factors instead of using state transformation. The dynamic error and residue stabilization of a non-linear faulty system have been discussed as well as the likelihood of secondary fault generation. The results indicate that the observer is able to determine fault-emergence, fault-disappearance and secondary fault formation well and quite fast.*

Key Words: *Observer Design, Troubleshooting, Fault Detection, Secondary Fault, Dynamic Error Linearization, Lipschitz Systems*

1. INTRODUCTION

In recent decades, many research studies have been drawn to fault-detection and system identification [1-5]. The presence of faults in a system leads to a lower value for efficiency, accuracy and speed, and, in some cases, even a complete breakdown. Thus, early fault detection is a major factor in efficiency and productivity of the procedure.

The ability to detect faults quickly, without the need for signal excitation, and to detect faults online have made the observer-based fault detection one of the most popular methods for fault detection in non-linear systems; hence, numerous efforts have been made in recent years to further develop the mentioned method.

Fault detection can be broadly classified into two categories, namely Model-based and Signal based. In the Model-based category, the accurate model of the system presented and any changes in the system parameters or fault occurrence have been studied by means of comparing of the faulty system with the healthy one. In the Signal-processing method, fault signature can be extracted from the measured signal of system [6-7].

Fault-detection using sliding-mode observer has been presented in refs. [8-9], and utilizing unknown input observer for fault detection can be found in Refs. [10-14]. Detecting faults using adaptive observer are studied in refs. [15-17]. High gain observers [18-21] have been used frequently in non-linear systems, and a few cases where the Kalman Filter has been used are presented in refs. [21-24].

Although substantial research has been undertaken on the observer-based fault detection, few or no studies have been conducted to investigate secondary fault generation or troubleshoot detection using observer-based approaches. This "lack of interest" on the part of the researchers is simply due to the fact that the observer's stability is not guaranteed while detecting secondary fault generation or the de-faulting method in a defective system, and as such, it should not be seen as insignificant. In other words, no research has been conducted to ascertain the observer's stability for defective systems or to stabilize the dynamic error and residue in nonlinear systems. The authors of this study think that linearizing dynamic error and residue enables both stabilizing the observer of a defective system and tracking the faulty system's behavior.

One of the most essential techniques for observer design is dynamic error linearization, which converts the non-linear system to an observable one by state transformation just as it converts the dynamic error to a linear form.

Krener and Isidori [25] and Bestel and Zeits [26] pioneered dynamic error linearization. Since then, as a topic of significant interest to a large number of researchers, multiple strategies for further developing it to various classes have been offered [27-29]. One of the most compelling arguments in favor of linearization is that it ensures the observer's stability during fault detection. The observer will be able to estimate system parameters even in the presence of a fault (assuming the fault does not result in system failure but just modifies operating parameters) and will be able to forecast fault erasure as well as the appearance of secondary faults. However, linearizing dynamic faults solely through state transformations is a lengthy procedure that requires performing complex and numerous arithmetic calculations (such as solving a system of partial differential equations), and even then, finding the appropriate coordinate transformations is not always possible [29, 30]. The approaches available are restricted to a subset of non-linear systems.

The requirement for state transition is the primary argument against such approaches. The disturbance and uncertainty are also transformed during state transformation, and the

knowledge regarding the nature of these variables is lost. The range and form of uncertainty as well as the order of disturbance are critical considerations in setting the fault-detection threshold, protecting the system from disturbance, and increasing the system's sensitivity to suspected problems. As a result, linearized dynamic error observers are rarely utilized for defect detection, state estimation, or parameter estimation in industrial systems, and are instead employed to structure and estimate the states of particular non-linear mathematical systems with limited classes.

The authors of this article developed a novel method for linearizing dynamic error that eliminates the necessity for state translation and linearizes non-linear components [31]. To linearize the dynamic error, the non-linear term that emerges from the dynamic error equation is expressed as a factor of the dynamic error in the estimated state term and the system output. Stabilizing the dynamic error requires stabilizing the matrix of coefficients in the dynamic error differential equation. As a result, the error differential equation is stabilized, and gain factors are shown as functions of the estimated state and system output. Indeed, the error differential equation is linearized using nonlinear gain factors.

The stability of such an observer is investigated in this study and in the continuation of ref. [31], and the requisite conditions for stabilizing the observer for residue tracking of a broken system to troubleshoot detection as well as secondary fault detection are demonstrated. Additionally, the estimation of fault and troubleshoot thresholds is detailed, and mathematical stabilization of the differential equation of dynamic error in faulty mode is demonstrated. The ability of the observer to detect defects in fault-free and defective systems as well as troubleshoot detection of a tunable micro capacitor subjected to nonlinear electrostatic force, are investigated and so is the behavior of residual and observer gains in faulty and fault-free modes.

2. Observer Design for the Nonlinear Lipchitz System

2.1. Observer construction and dynamic error linearization

This section will demonstrate the aforementioned observer's ability to linearize dynamic error and stabilize the residual in the presence of faults. The whole technique for designing an observer is described in ref [31]. To maintain the integrity and completeness of the fault detection process, a brief description of the observer design will be provided.

The procedure is based on the transformation of non-linear terms into elements of the dynamic error in the variable that is dependent on the estimated state and output. This approach converts the system of differential equations governing dynamic error to a matrix of coefficients (in terms of the estimated state and output) and then stabilizes it before constructing the observer and determining its gains.

To begin, the technique is provided with the assumption that there are no uncertainties in the system.

Take the following non-linear system as an example:

$$\dot{x} = Ax + \varphi(x,u)$$
$$y = Cx \qquad (1)$$
$$\dot{x} = \frac{dx}{dt}$$

in which, $x \in R^n$, $u \in R^r$, and $y \in R^m$ represent state, known input and the system output, respectively. In the above equation $A \in R^{n \times n}$ and $C \in R^{m \times n}$ are system matrices of known and constant value. The function $\varphi(x,u) \in R^n$ is a continuous, vector function of non-infinity extremes, i.e. it satisfies the Lipschitz condition [32]:

$$\left\| \varphi\left(x_1, u\right) - \varphi\left(x_2, u\right) \right\| \leq \gamma \left\| x_1 - x_2 \right\| \tag{2}$$

in which, γ is a positive value denoting the Lipschitz coefficient of $\varphi(x,u)$. Following observer is considered for estimating the state of the system (1):

$$\dot{X} = AX + \varphi\left(X, u\right) + L\left(X, y\right)\left(y - Y\right)$$
$$Y = CX \tag{3}$$

in which, $X \in R^n$ and $Y \in R^m$ represent the estimated state and the system output, respectively. $L(X,y) \in R^{m \times n}$ is the matrix of the observer gains, and it should be chosen in such a way that the dynamic error remains steady. (For the purpose of simplicity, $L(X,y)$ will be written as L. Naturally, in addition to estimating the state, observer (3) can also estimate the system output.

The following requirements must be followed in order to calculate the observer's gains [31]:

- Matrices A and C must be observable, i.e., matrix $[ACA \ldots CA^{n-1}]^T$ must be of full rank.
- Matrix C must be of full rank.
- The non-linear term $\varphi(x,u)$ must be uniquely determinable using the system output [31].

Now, assuming the state error to be $e = x - X$, the system of differential equations for error is determined as follows:

$$\dot{e} = \left(A - LC\right)e + \varphi\left(x, u\right) - \varphi\left(X, u\right) \tag{4}$$

In order to design the observer, L should be determined so that the dynamic errors are asymptotically stable.

Lemma. If matrix $F(y,X,u) \in R^{n \times n}$ can be determined in such a way that satisfies the below equation, then the error vector is asymptotically stable, given the matrix $[A-LC+F(y,X,u)]$ is negative-definite [31].

$$F\left(y, X, u\right)\left(x - X\right) = \varphi\left(x, u\right) - \varphi\left(X, u\right) \tag{5}$$

Stabilizing the matrix $[A-LC+F(y,X,u)]$, the observer's gains are calculable. The total of the elements on the main diagonal (trace of $[A-LC+F(y,X,u)]$) must be negative in order to stabilize the observer. Even and odd submatrices must have positive and negative determinants, respectively. This enables the determination of the observer gains to be made easily. The observer gains are determinable. Under such circumstances, the elements of $F(y,X,u)$ are presented as part of the observer gains, and ultimately, the matrix $[A-LC+F(y,X,u)]$ is presented as a constant matrix independent of u, X, and y and the differential equation of dynamic error is linearized. The dynamic error approaches zero with an exponential rate and the convergence rate is determined as desired.

Thus, determining $F(y,X,u)$ seems to be the most challenging aspect of the whole procedure since all other tasks in the observer design are relatively straightforward. Two explicit methods for determining $F(y,X,u)$ have been presented in Ref. [31].

2.2. Ability of the observer to determine faults and categorizing the faults in the actuator and dynamic system

The preceding section discusses the observer design technique for estimating output and system state. The dynamic error can be linearized using the gain factors that depend on the estimated state and output using the procedure described above. On this basis, the present part examines the stability of the error and residue following the appearance of defects in the system and determines the residue range for the defective condition. These are the detection thresholds for faults. The following conditions are required for system troubleshooting and secondary fault detection:

- The dynamical system remains stable notwithstanding the emergence of primary and secondary faults. It is self-evident that no observer can detect an unstable system.
- System stability should be guaranteed in the presence of uncertainty and disturbance. In other words, the value of the mentioned parameters should be in a range that does not cause any instability in microstructure.
- Qualitative form of differential equation of dynamic error or governing dynamic equation of dynamical system should be untouched after fault emergence. For example, the size of A and C matrices should not be changed or primary form of (x) should be fixed, but their magnitude can be changed. For example, neither the size of A and C matrices nor their fundamental form should be changed, but their magnitude can be adjusted. For example, matrix A can be changed from [0 1] to [2 3] but it should not be changed to [0 1 0]. Or $(x,)$ can be changed from $2\sin(x)$ to $3\sin(x)$ but it should not be changed from $2\sin(x)$ to x^2.

Now, consider the dynamic system:

$$\dot{x} = Ax + \varphi(x,u) + E_1 f_1$$
$$y = Cx \tag{6}$$

in which, $f_1 \in R^p$ and $E_1 \in R^{n \times p}$ denotes the fault and characteristics matrix, respectively (note that there are no null or zero elements in f_1). If observer (3) is used to determine the output and residue of system (6), the system of differential equations for dynamic error may be presented as:

$$\dot{e} = Ke + E_1 f_1$$
$$e(t_1) = e_1 \tag{7}$$

in which, K is a negative definite matrix, and is determined by stabilizing $[A-LC+F(y,X,u)]$. Note that K is not uniquely determined; t_1 and e_1 represent the time of fault formation and the value of the dynamic error in that time, respectively. Considering $y=Cx$ and Eq. (7), the residue dynamic equation is derived as the following:

$$\dot{r} = Dr + E_{1C} f_1$$
$$r(t_1) = r_1 \tag{8}$$

in which, $D=CK$ and $E_{1C}=CE_1$, while r_1 is the residue at the time of fault emergence. The residue response for the above equation is:

$$r(t) = \exp\left[D(t-t_1)\right]\left\{r_1 + \int_{t_1}^{t} E_{1C} f_1(\tau) \exp\left[-D(\tau-t_1)d\tau\right]\right\} \tag{9}$$

If $E_{1C}f_1(\tau)$ satisfies $F_{1d} \leq E_{1C} \leq F_{1u}$, the dynamic response limits are determined as:

$$r(t) = \exp\left[D(t-t_1)\right]\left(r_1 + D^{-1}F_{1u}\right) - D^{-1}F_{1u}$$
$$r(t) = \exp\left[D(t-t_1)\right]\left(r_1 + D^{-1}F_{1d}\right) - D^{-1}F_{1d} \tag{10}$$

Now, since K is negatively definite and $t_1 > t$, the residue steady response is bound by $-D^{-1}F_{1u}$ and $-D^{-1}F_{1d}$. In fact, these ranges demonstrate the upper and lower limit for detecting the fault f_1 after formation.

Now, suppose that at time t_2, fault f_2 is formed in the defective system (6). Or:

$$\dot{x} = Ax + \varphi(x,u) + E_1 f_1 + E_2 f_2$$
$$y = Cx \tag{11}$$

in which, $f_2 \in R^q$ and $E_2 \in R^{n \times q}$ represent the secondary fault and the secondary fault matrix (note that there are no zero elements in f_2). If observer (3) is to be used in order to estimate the output and residue of system (11), the system of differential equations for dynamic error and residue may be presented as:

$$\dot{e} = Ke + E_1 f_1 + E_2 f_2$$
$$e(t_2) = e_2$$
$$\dot{r} = Dr + E_{1C} f_1 + E_{2C} f_2$$
$$r(t_2) = r_2 \tag{12}$$

in which, e_2 and r_2 represent the value of the dynamic error and residue for $t > t_2$. Also, $E_{2C} = CE_2$. For Eq. (12), residue response for $t > t_2$ is:

$$r(t) = \exp\left[D(t-t_2)\right]\left\{r_2 + \int_{t_2}^{t} \left(E_{1C} f_1(\tau) + E_{2C} f_2(\tau)\right) \exp\left[-D(\tau-t_2)\right]d\tau\right\} \tag{13}$$

If $E_{1C}f_1(\tau) + E_{2C}f_2(\tau)$ satisfies $F_{2d} \leq E_{1C}f_1(\tau) + E_{2C}f_2(\tau) \leq F_{2u}$, the dynamic response limits are determined as:

$$r(t) = \exp\left[D(t-t_2)\right]\left(r_2 + D^{-1}F_{2u}\right) - D^{-1}F_{2u}$$
$$r(t) = \exp\left[D(t-t_2)\right]\left(r_2 + D^{-1}F_{2d}\right) - D^{-1}F_{2d} \tag{14}$$

Now, since K is negatively definite and $t > t_2$, the residue steady response is bound by $-D^{-1}F_{2u}$ and $-D^{-1}F_{2d}$. Note that $E_1 f_1 = -E_2 f_2$ denotes de-faulting (troubleshoot).

As can be observed, linearizing dynamic error and the residue enables the residue to be stabilized in the presence of a defect, which enables secondary fault identification and troubleshooting.

This section established the observer's stability in the presence of faults, assuming no uncertainty or turbulence. When there is uncertainty or disturbance in the system, the problem can be handled without sacrificing its general utility; in this situation, the ranges of disturbance and uncertainty should be indicated in Eqs. (6) and (7). In other words, when

computing the residue ranges in Eqs. (9) and (10), it is necessary that the ranges for disturbance and uncertainty be added to $F_{1d} \leq E_1 c f_1(\tau) + U + N \leq F_{1u}$ and $F_{2d} \leq E_1 c f_1(\tau) + E_2 c f_2(\tau) + U + N \leq F_{2u}$, in which U and N represent uncertainty and disturbance.

3. RESULTS AND DISCUSSION

3.1. Model description of the case study (micro tunable capacitor subjected to nonlinear electrostatic force)

A parallel plate capacitor is depicted schematically in Fig. 1a [33]. It comprises a moveable electrode hung above a stationary conductor plate. Between two electrodes, the major gap is G_1. Electrostatic attraction caused by the applied bias voltage u pushes the moveable electrode towards the fixed plate. The top view of the movable electrode, which is suspended by four supporting beams, is shown in Fig. 1b (two at each side). S and h denote the area and thickness of the moveable electrode, respectively. The width, thickness, and length of beams are denoted by the symbols b, h, and L. Each beam has an equivalent rigidity of $K = 12EIL^{-3}$ where E and I are, respectively, the Young's modulus and the cross section moment of inertia. With a density of ρ, the movable electrode is termed isotropic.
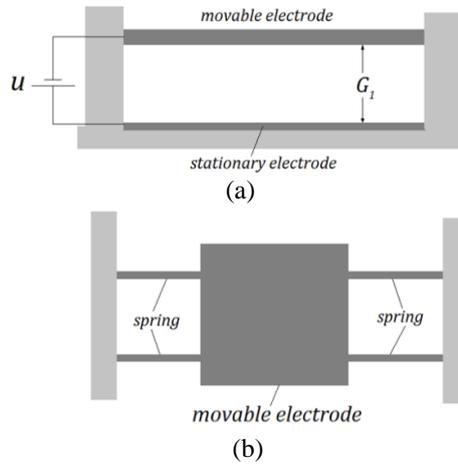
Fig. 1 Micro tunable capacitor; a) Capacitor from side view, b) Capacitor from top view

Governing dynamic equation of movable electrode of capacitor is as:

$$m\frac{d^2z}{dt^2} + c'\frac{dz}{dt}z + kz = \frac{\varepsilon_0 A u^2}{2(G_1 - z)^2} \tag{15}$$

where $m = \rho A h, c', k = 4K$ are mass, damping coefficient and resultant spring constant, respectively, t is time and $\varepsilon_0 = 8.854 \times 10^{-12}$ $C^2 N^{-1} m^{-2}$ is permittivity of vacuum; z is deflection of movable electrode. Physical and geometrical properties of studied micro capacitor are presented in Table 1.

For convenience, Eq. (15) may be rewritten in a non-dimensional form by defining the following parameters [34]:

$$x = \frac{z}{G_1}, \ c = \frac{c'}{kt^*}, \ \alpha = \frac{\varepsilon_o A}{2kG_0^3}, \ t^* = \sqrt{\frac{m}{k}}, \ \tau = \frac{t}{t^*} \tag{16}$$

where x, c, τ are dimensionless deflection, damping, and time. α is dimensionless parameter of electrostatic force. Therefore, Eq. (15) can be written as:

$$\frac{d^2 x}{dt^2} + c \frac{dx}{dt} + x = \frac{\alpha u^2}{(1-x)^2} \tag{17}$$

Table 1 Physical and geometrical properties of micro capacitor

Area of movable electrode	A=400μm×400μm
Young modulus	E=169 GPa
Length of each supporting beam	L=100 μm
Width of supporting beam	b=5 μm
Thickness of supporting beam	h=1 μm
Primary gap between two electrodes	G_1=4 μm
Density	ρ=2300 Kg/m^3

Eq. (17) can be presented is state space form as:

$$\begin{cases} \begin{bmatrix} \dot{x}_1 \\ \dot{x}_2 \end{bmatrix} = \begin{bmatrix} 0 & 1 \\ -1 & -c' \end{bmatrix} \begin{bmatrix} x_1 \\ x_2 \end{bmatrix} + \begin{bmatrix} 0 \\ \dfrac{\alpha u^2}{(1-x_1)^2} \end{bmatrix} \\ \\ y = \begin{bmatrix} 1 & 0 \end{bmatrix} \begin{bmatrix} x_1 \\ x_2 \end{bmatrix} \end{cases} \tag{18}$$

Considering disturbance, uncertainty and fault vector, Eq. (18) is altered as:

$$\begin{cases} \begin{bmatrix} \dot{x}_1 \\ \dot{x}_2 \end{bmatrix} = \begin{bmatrix} 0 & 1 \\ -1 & -c' \end{bmatrix} \begin{bmatrix} x_1 \\ x_2 \end{bmatrix} + \begin{bmatrix} 0 \\ \dfrac{\alpha u^2}{(1-x_1)^2} \end{bmatrix} + \delta \begin{bmatrix} 0 \\ \dfrac{\alpha n^2 u^2}{(1-x_1)^2} \end{bmatrix} + \delta' \begin{bmatrix} 0 \\ \sin t \end{bmatrix} + \begin{bmatrix} 0 \\ 1 \end{bmatrix} \dfrac{\alpha(n^2-1)u^2}{(1-x_1)^2} \\ \\ y = \begin{bmatrix} 1 & 0 \end{bmatrix} \begin{bmatrix} x_1 \\ x_2 \end{bmatrix} \end{cases} \tag{19}$$

where $x_1 = x$ and $x_2 = dx_1/dt$, $\delta[0 \ \alpha n^2 u^2/(1-x_1)^2]^T$, $\delta'[0 \ \sin t]^T$, $\alpha(n^2-1)u^2/(1-x_1)^2[0 \ 1]^T$ are uncertainty, disturbance and fault vectors, respectively. The simulated fault is abrupt decreasing of the applied voltage which related by n in fault vector. For the fault-free system $n=1$ and for faulty system $0 \leq n < 1$, following observer is considered for output estimation and residual generation of system (19).

$$\begin{cases} \begin{bmatrix} \dot{X}_1 \\ \dot{X}_2 \end{bmatrix} = \begin{bmatrix} 0 & 1 \\ -1 & -c' \end{bmatrix} \begin{bmatrix} X_1 \\ X_2 \end{bmatrix} + \begin{bmatrix} 0 \\ \dfrac{\alpha u^2}{(1-X_1)^2} \end{bmatrix} + \begin{bmatrix} L_1 \\ L_2 \end{bmatrix} (y-Y) \\ \\ r = y - Y \end{cases} \tag{20}$$

where L_1 and L_2 are observer gains. With subtracting of Eq. (19) from Eq. (20), equation of dynamic error is extracted as:

$$\begin{bmatrix} \dot{e}_1 \\ \dot{e}_2 \end{bmatrix} = \begin{bmatrix} 0 & 1 \\ -1 & -c' \end{bmatrix} \begin{bmatrix} e_1 \\ e_2 \end{bmatrix} + \begin{bmatrix} 0 \\ \dfrac{\alpha u^2}{(1-x_1)^2} - \dfrac{\alpha u^2}{(1-X_1)^2} \end{bmatrix} - \begin{bmatrix} L_1 \\ L_2 \end{bmatrix} (y-Y)$$

$$+\delta \begin{bmatrix} 0 \\ \dfrac{\alpha n^2 u^2}{(1-y)^2} \end{bmatrix} + \delta' \begin{bmatrix} 0 \\ \sin t \end{bmatrix} + \begin{bmatrix} 0 \\ 1 \end{bmatrix} \dfrac{\alpha(n^2-1)u^2}{(1-x_1)^2} \tag{21}$$

Attention to $y=x_1$ and using proposed method for construction of F matrix [31] we have:

$$F = \begin{bmatrix} 0 & 0 \\ \alpha u^2 \dfrac{2-(X_1+y)}{\left[(1-y)(1-X_1)\right]^2} & 0 \end{bmatrix} \tag{22}$$

So Eq. (21) can be rewritten as:

$$\begin{bmatrix} \dot{e}_1 \\ \dot{e}_2 \end{bmatrix} = \begin{bmatrix} -L_1 & 1 \\ \alpha u^2 \dfrac{2-(X_1+y)}{[(1-y)(1-X_1)]^2} -1 - L_2 & -c \end{bmatrix} \begin{bmatrix} e_1 \\ e_2 \end{bmatrix}$$

$$+\delta \begin{bmatrix} 0 \\ \dfrac{\alpha n^2 u^2}{(1-y)^2} \end{bmatrix} + \delta' \begin{bmatrix} 0 \\ \sin t \end{bmatrix} + \begin{bmatrix} 0 \\ 1 \end{bmatrix} \dfrac{\alpha(n^2-1)u^2}{(1-y)^2} \tag{23}$$

Stabilizing the coefficient matrix in Eq. (23) is required to determine the observer gains. Through the stabilization of the coefficient matrix (for the stabilizing of the mentioned matrix, the even and odd sub matrices of the coefficient matrix must be positive and negative, respectively). Observer gains were calculated using this approach and are shown in the following equation:

$$L_1 = \varepsilon_1 - c$$

$$L_2 = \varepsilon_2 - 1 - L_1 c + \dfrac{2-(X_1+y)}{[(1-y)(1-X_1)]^2} \alpha u^2 \tag{24}$$

$$L_2 = \varepsilon_2 - 1 - (\varepsilon_1 - c)c + \dfrac{2-(X_1+y)}{[(1-y)(1-X_1)]^2} \alpha u^2$$

where ε_1 and ε_2 are positive numbers. By inserting the observer gains, the matrix of $A-LC+F$ is extracted as follows:

$$A-LC+F = \begin{bmatrix} c-\varepsilon_1 & 1 \\ -\varepsilon_2 + c(\varepsilon_1-c) & -c \end{bmatrix} \tag{25}$$

### 3.2. Results of output estimation and fault detection

In this section, the obtained results for fault detection, fault release, and fault detection of faulty micro tunable capacitor are presented. For this simulation $u=3V$, $\varepsilon_1=2$, $\varepsilon_2=1$ are intended. In this paper, the thresholds of a healthy system are shown with dot-dot (….). The thresholds of initial and secondary fault detection are line-line (----) and line-dot (-.-.-), respectively. A fault is considered as reduction of applied voltage.

The thresholds for determining of the fault size for $|\delta|<0.1$ and $|\delta'|<0.003$ are determined and shown in Table 2.

Table 2 The upper and lower thresholds for different magnitude of n for $|\delta|<0.1$ and $|\delta'|<0.003$

| n	Upper threshold	Lower threshold
$n=1$	0.006392	-0.006392
$n=0.9$	-0.0001622	-0.01211
$n=0.8$	-0.005673	-0.01722
$n=0.7$	-0.01054	-0.02173
$n=0.6$	-0.01475	-0.02564
$n=0.5$	-0.01832	-0.02895
$n=0.4$	-0.02123	-0.03166
$n=0.3$	-0.0235	-0.03377
$n=0.2$	-0.02512	-0.03527
$n=0.1$	-0.0261	-0.03617
$n=0$	-0.02642	-0.03647

The results of initial fault detection for various amounts of δ' are shown in Figs. 2 to 4. The fault is considered as voltage decreasing where at $t=6.2\times10^{-3}$s magnitude of $n=1$ abruptly decreased to $n=0.7$. As can be seen from these figures, the observer is able to determine the size of the fault for different magnitude of δ'. Also, it can be seen from this figure that an abrupt change of residual is observed as soon as a fault occurs. And the residual is settled in the bound of relevant threshold.
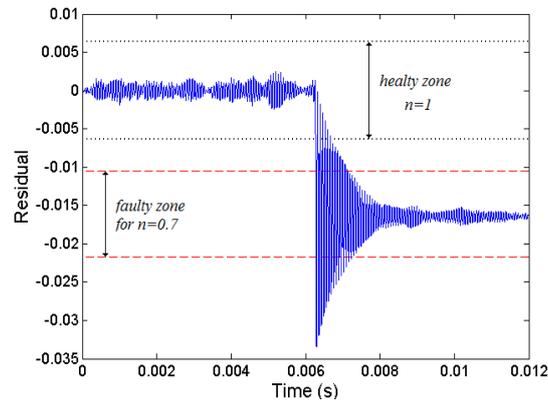
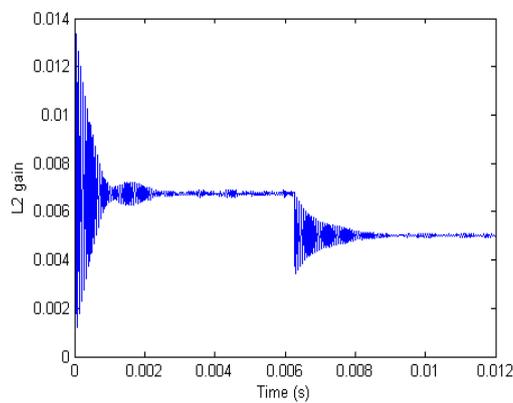**Fig. 2** Fault detection result for $n=0.7$ and $\delta'=0$
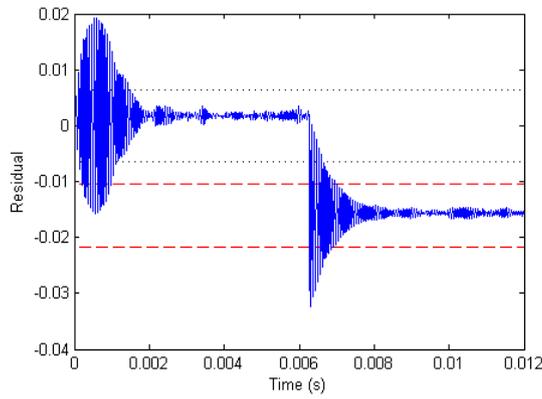
Fig. 3 Fault detection result for n=0.7 and δ'=0.003
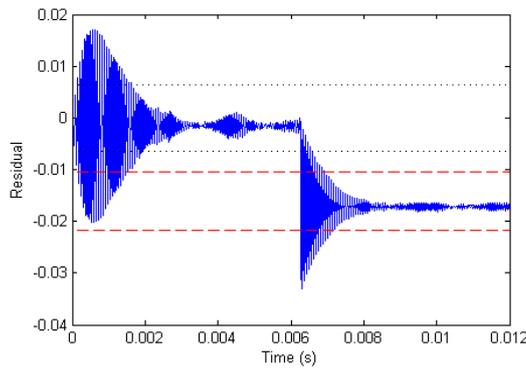
Fig. 4 Fault detection result for n=0.7 and δ'=-0.003

Fig. 5 also shows the time depending variation of gain L_2. As shown in this figure, as soon as a fault occurs, the coefficient of L_2 changes significantly and after a short time, converges to


Fig. 5 Time dependent variation of L_2 for n=1 (t<6.2×10^{-3}s), n=0.7(t≥6.2×10^{-3}s) and δ'=-0.003

near 0.005. Considering Figs. 2 to 5, it is obvious that residual and observer gain have similar shapes. They have considerable change after fault occurrence and also converge to specific magnitude.

Now consider that at t=6.2×10^{-3}s the applied voltage change from $1u(n=1)$ to $0.7u$ (n=0.7) and at t=12.4×10^{-3}s the actuator fault is released and the voltage is increased from $0.7u$ to $1u$ (troubleshoot).

For this situation, after fault is released, the residual must be settled in healthy threshold zone. Fig. 6 illustrates this condition for δ'=0.05. As shown in this figure the presented observer has a good ability for detecting the fault occurrence and troubleshooting. Fig. 7 shows change of L_2 *versus* time. Also, in this case a meaningful similarity can be observed in the behavior of Figs. 6 and 7.
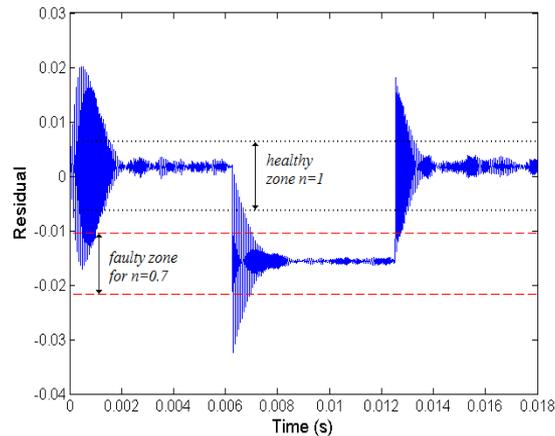

**Fig. 6** Fault and troubleshoot detection for n=0.7 and δ'=0.05
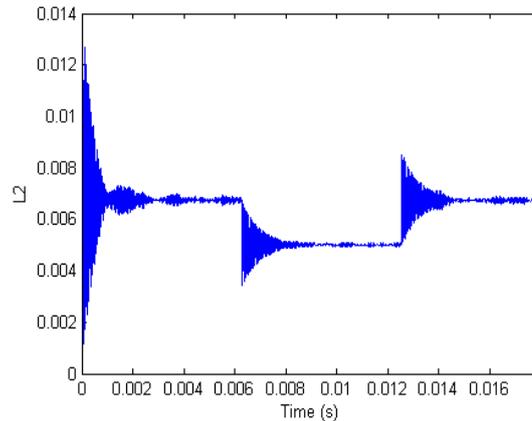
Fig. 7 Variation of L_2 for simulation of Fig. 6

In the continuation of this section, we intend to examine the observer's ability for secondary fault detection. It means that initially a fault has occurred in the system, and then another fault occurs in the faulty system. For example, at $t=6.2\times10^{-3}$s the applied voltage decreases from $1u$ to $0.7u$, and then at $t=12.4\times10^{-3}$s the applied voltage decreases from $0.7u$ to zero.

Fig. 8 shows the simulation results for such a situation. As it is obvious from this figure, the observer is able to detect a secondary fault in the system at an acceptable speed and can accurately calculate the secondary fault level. As can be seen in Fig. 9, after the formation of the primary and secondary faults, L_2 changes substantially.
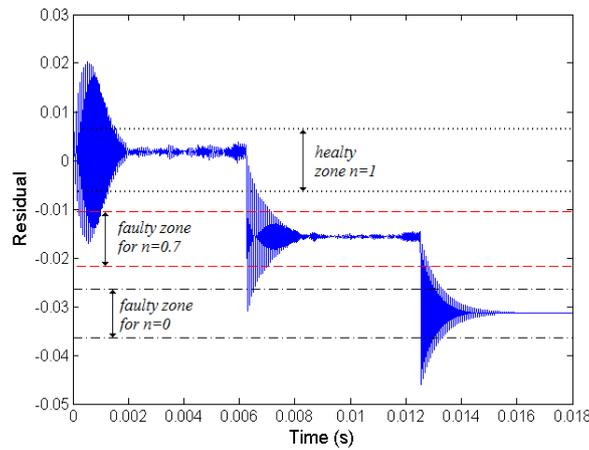
Fig. 8 The initial ($n=0.7$) and secondary ($n=0$) fault defection using proposed observer
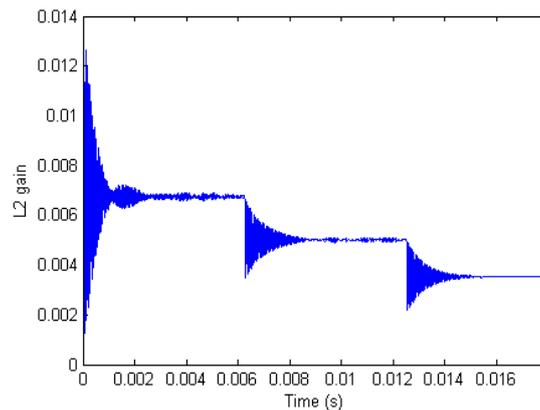
Fig. 9 Time dependent variation of L_2 for simulation results of Fig. 8

4. CONCLUSION

Troubleshooting and the creation of secondary defects in already problematic systems were studied in this research utilizing observer-based methodologies due to their relative relevance. To accomplish this, an observer capable of linearizing the differential equation

of dynamic error and residue was used. It was demonstrated that the linearization approach used ensures the observer's stability in the presence of faults and enables tracking of the residue's behavior even after the onset of faults in order to assess fault disappearance or the generation of secondary faults. The proposed observer design approach does not require state transformation and is based on rewriting the error differential equation non-linearity in terms of a non-linear term dependent on the estimated state and output. Additionally, the necessary circumstances for the construction and stabilization of observers were discussed. Finally, the observer's capacity to detect fault creation, troubleshoot, and the onset of secondary faults was investigated.

The system under investigation comprised a micro tunable capacitor that was subjected to an electrostatic force that was non-linear. The results demonstrate that the observer is capable of accurately determining fault emergence, fault disappearance, and secondary fault creation. Additionally, it was demonstrated that when flaws manifest, a dramatic change in L_2 can be noticed.

REFERENCES

1. Isermann, R., 2006, *Fault-diagnosis systems: an introduction from fault detection to fault tolerance,* Springer Science & Business Media.
2. Čiča, Đ., Zeljković, M., Tešić, S., 2020, *Dynamical contact parameter identification of spindle-holder-tool assemblies using soft computing techniques*, Facta Universitatis-Series Mechanical Engineering, 18(4), pp. 565-577.
3. Mellit, A., Tina, G.M., Kalogirou, S.A., 2018, *Fault detection and diagnosis methods for photovoltaic systems: A review*, Renewable and Sustainable Energy Reviews, 91, pp. 1-17.
4. Attaran, B., Ghanbarzadeh, A., 2015, *Bearing Fault Detection Based on Maximum Likelihood Estimation and Optimized ANN Using the Bees Algorithm*, Journal of Applied and Computational Mechanics, 1(1), pp. 35-43.
5. Wu, R.T., Jahanshahi, M.R., 2020, *Data fusion approaches for structural health monitoring and system identification: past, present, and future*, Structural Health Monitoring, 19(2), pp. 552-586.
6. Alzghoul, A., Jarndal, A., Alsyouf, I., Bingamil, A.A., Ali, M.A., AlBaiti, S., 2021, *On the Usefulness of Pre-processing Methods in Rotating Machines Faults Classification using Artificial Neural Network*, Journal of Applied and Computational Mechanics, 7(1), pp. 254-261.
7. Jahangiri, M., Roknizadeh, S.A.S., 2018, *Clogged impeller diagnosis in the centrifugal pump using the vibration and motor current analysis,* Journal of Applied and Computational Mechanics, 4(4), pp. 310-317.
8. Hamdi, H., Rodrigues, M., Mechmeche, C.H., Braiek, N.B., 2019, *Fault diagnosis based on sliding mode observer for LPV descriptor systems*, Asian Journal of Control, 21(1), pp. 89-98.
9. Ríos, H., Punta, E., Fridman, L., 2017, *Fault detection and isolation for nonlinear non-affine uncertain systems via sliding-mode techniques*, International Journal of Control, 90(2), pp. 218-230.
10. Triki, I., Massaoud, R.B., Bouani, F., 2020, *Unknown Input Observer-Based Design for a Class of Nonlinear System with Time-Variable Delay*, Journal of Control, Automation and Electrical Systems, 31(5), pp. 1097-1107.
11. Zhou, M., Wang, Z., Shen, Y., 2017, *Fault detection and isolation method based on $H−/H∞$ unknown input observer design in finite frequency domain*, Asian Journal of Control, 19(5), pp. 1777-1790.
12. Xu, F., Tan, J., Wang, X., Puig, V., Liang, B., Yuan, B., 2017, *Mixed active/passive robust fault detection and isolation using set-theoretic unknown input observers*, IEEE Transactions on Automation Science and Engineering, 15(2), pp. 863-871.
13. Mobki, H., Sadeghi, M. H., Rezazadeh, G., 2015, *Design of Direct Exponential Observers for Fault Detection of Nonlinear MEMS Tunable Capacitor*, IJE TRANSACTIONS A: Basics, 28(4), pp. 634-641.
14. Tolouei, H., Shoorehdeli, M.A., 2021, *Nonlinear Parity Approach to Fault Detection in Nonlinear Systems Using Unknown Input Observer*, Iranian Journal of Science and Technology, Transactions of Electrical Engineering, 45, pp. 321-333.
15. Chatterjee, S., Sadhu, S., Ghoshal, T.K., 2017, *Improved estimation and fault detection scheme for a class of non-linear hybrid systems using time delayed adaptive CD state estimator*, IET Signal Processing, 11(7), pp. 771-779.

16. Kazerooni, M., Khayatian, A., Safavi, A., 2018, *Fault estimation for a class of interconnected non-linear systems with time-varying delay using robust adaptive unknown input observers*, IMA Journal of Mathematical Control and Information, 35(1), pp. 231-247.
17. Sinha, V., Mondal, S., 2021, *Adaptive unknown input observer approach for multi-fault diagnosis of PEM fuel cell system with time-delays,* Journal of Control and Decision, 8(2), pp. 222-232.
18. Boum, A.T., Talla, S., 2019, *High gain observer and moving horizon estimation for parameters estimation and fault detection of an induction machine: A comparative study*, Journal of Control & Instrumentation, 8(2), pp. 15-26.
19. Ma, H.J., Liu, Y., Li, T., Yang, G.H., 2018, *Nonlinear high-gain observer-based diagnosis and compensation for actuator and sensor faults in a quadrotor unmanned aerial vehicle*, IEEE Transactions on Industrial Informatics, 15(1), pp. 550-562.
20. Trejo, D.R.E., Taheri, S., Sánchez, J.A.P., 2019, *Switch fault diagnosis for boost DC–DC converters in photovoltaic MPPT systems by using high-gain observers*, IET Power Electronics, 12(11), pp. 2793-2801.
21. Baranowski, J., Bania, P., Prasad, I., Cong, T., 2017, *Bayesian fault detection and isolation using Field Kalman Filter*, EURASIP Journal on Advances in Signal Processing, 2017, 79.
22. Faraji, A., Nejati, Z., Abedi, M., 2020, *Actuator Faults Estimation for a Helicopter UAV in the Presence of Disturbances*, Journal of Control, Automation and Electrical Systems, 31, pp. 1153-1164.
23. Zarei, J., Kowsari, E., Razavi-Far, R., 2018, *Induction motors fault detection using square-root transformed cubature quadrature Kalman filter*, IEEE Transactions on Energy Conversion, 34(2), pp. 870-877.
24. Liu, L., Zhu, J., Lei, Y., 2021, *A Generalized Identification of Joint Structural State and Unknown Inputs Using Data Fusion MKF-UI*, Journal of Applied and Computational Mechanics, 2021. 7, pp. 1198-1204.
25. Krener, A.J., Isidori, A., 1983, *Linearization by output injection and nonlinear observers*, Systems & Control Letters, 3(1), pp. 47-52.
26. Bestle, D., Zeitz, M. 1983, *Canonical form observer design for non-linear time-variable systems*, International Journal of control, 38(2), pp. 419-431.
27. Califano, C., Moog, C.H., 2014, *The observer error linearization problem via dynamic compensation*, IEEE Transactions on Automatic Control, 59(9), pp. 2502-2508.
28. Lee, H.G., Kim, K.D., Jeon, H.T., 2015, *Restricted dynamic observer error linearizability*, Automatica, 53, pp. 171-178.
29. Lee, H.G., 2017, *Verifiable conditions for multioutput observer error linearizability*, IEEE Transactions on Automatic Control, 62(9), pp. 4876-4883.
30. Lynch, A.F., Bortoff, S.A., 1997, *Non-linear observer design by approximate error linearization*, Systems & Control Letters, 32(3), pp. 161-172.
31. Mobki, H., Sadeghi, M.H., Eskandari, M.M., 2020, *A New Procedure for Linearizing Dynamic Error and Establishing Absolute Robustness to Lipschitz Nonlinearity*, Journal of Control, Automation and Electrical Systems, 31, pp. 625-635.
32. Mobki, H., Sadeghi, M.H., Rezazadeh, G., 2015, *Application of Thau observer for fault detection of micro parallel plate capacitor subjected to nonlinear electrostatic force*, International Journal of Engineering, 28(2), pp. 270-276.
33. Mobki, H., Sadeghi, M.H., Rezazadeh, G., 2015, *State estimation of MEMs capacitor using Taylor expansion*, International Journal of Engineering, 28(5), pp. 764-770.
34. Mobki, H., Majidzadeh Sabegh, A., Azizi, A., Ouakad, H.M., 2020, *On the implementation of adaptive sliding mode robust controller in the stabilization of electrically actuated micro-tunable capacitor*, Microsystem Technologies, 26, pp. 3903-3916.